RSC Advances

ROYAL SOCIETY OF CHEMISTRY

www.rsc.org/advances

RSC Advances

ARTICLE

Size evolution and ligand effects on the structures and stability of $(AuL)_n$ (L = Cl, SH, SCH_3, PH_2, $P(CH_3)_2$, *n* = 1-13) clusters†

Received 00th January 20xx,
Accepted 00th January 20xx

DOI: 10.1039/x0xx00000x

www.rsc.org/

Yao Liu,[a] Zhimei Tian[a] and Longjiu Cheng[a*]

The synthesis and characterization of ligand protected gold nanoclusters (Au_mL_n) have attracted great interests. After the crystalizations of $Au_{102}(SR)_{44}$ and $Au_{25}(SR)_{18}^-$ clusters, the syntheses and theoretical predictions of Au_mL_n clusters have been greatly accelerated. To date, there are few systematic studies on the size evolution and ligand effects of Au-L binary systems. Here, taking stoichiometric $(AuL)_n$ (*n* = 1-13) system as a test case, we theoretically investigated the ligand effects (L = Cl, SH, SCH_3, PH_2, $P(CH_3)_2$) on the structures and size evolution. The method of genetic algorithm combined with density functional theory is used to perform extensive global search of the potential energy surface to locate the global minima (GM) and low-lying isomers. For each ligand, the structural features are roughly similar to $(AuSR)_n$, that is, the GMs change from single ring to catenane structures. Besides, a new folding way (ring-at-ring) is revealed in the GMs at *n* = 12-13. The GM structures are very similar for L = SH and SCH_3 and for L = PH_2 and $P(CH_3)_2$, indicating that the R groups can be directly replaced by H in calculations. However, there are obvious differences on the GM structures for L = Cl, SH and PH_2. It is found that the origin of the ligand effects is the polarity of Au-L bond. Au-Cl bond is of the highest plorarity, and noncovalent interaction index approach reveals that the Au···Au aurophilic interaction is the strongest for L = Cl, followed by L = SH and L = PH_2. Moreover, the polarity of Au-L bond may affect the preferred Au-L-Au bond angle, which is an important geometric parameter. The linearity of Cl-Au-Cl in is the easiest to be broken for more Au···Au contacts, which is viewed in the GMs of $(AuCl)_n$ at *n* = 7, 8 and 12.

I. Introduction

Ligand-protected gold nanoparticles (Au_mL_n) have attracted considerable interest because of their promising applications in nanocatalysis, medicine and optical devices.[1-7] Among Au_mL_n clusters, thiolate protected gold nanoclusters $Au_m(SR)_n$ are the most studied systems. Two breakthroughs of $Au_m(SR)_n$ clusters are the crystal structure determinations of $Au_{102}(SR)_{44}$ and $Au_{25}(SR)_{18}$ clusters, which consist of $Au_n(SR)_{n+1}$ (*n*=1, 2) oligomers that bind to a gold core with high symmetry.[8, 9] Then based on this model of a gold core surrounded by gold thiolate oligomers, density functional theory (DFT) calculations was used to predict the structures of $Au_{38}(SR)_{24}$,[10-14] $Au_{24}(SR)_{20}$,[15, 16] and $Au_{144}(SR)_{60}$.[17-21] Recent research found that $Au_{68}(SR)_{30}$ cluster and $Au_{18}(SC_6H_{11})_{14}$ was still consistent with this model of a gold core surrounded by gold thiolate oligomers.[22-24] Meanwhile, several experimental studies have revealed the ligand effects on the stabilities and properties of noble metal clusters. The redox properties of $Au_{38}(SPhX)_{24}$ clusters and the original magic stability of $Au_m(SR)_n$ clusters was demonstrated by employing the ligand effects.[25, 26] Recently, Johnson *et al.*[27] studied the effect of phosphines substitution on ligand reactivity and binding, and it is shown that several larger clusters readily undergo exchange of PPh_3 ligands in solution for singly substituted PPh_2Me and PPh_2Cy ligands. With the experimental observations on the ligand effects on Au nanoclusters, many theoretical calculations have been performed to understand how surface ligands influence on the electronic structure and stability of metal nanoclusters. Ligand effects on the structure and electronic optical properties of $Au_{25}(SR)_{18}^-$ clusters have been explored and the work revealed that *p*-thiophenolates ligands that include electron-withdrawing groups could result in distortion of the $Au_{25}S_{18}$ framework.[28] $Au_{38}(SR)_{24}$, $Au_{102}(SR)_{44}$ and $Au_{24}(SR)_{20}$ have been also performed to study the ligand effects on the stability, and found that -SPhCOOH was more favorable binding than -SPh and -SPhF.[29-32] Recently, the role of the anchor atom and ligand types on the properties of $Au_m(SR)_n$ nanoclusters have been performed, and there was a more pronounced effect on the gold–ligand unit structure and ultimately the aurophilic interactions.[33, 34]

[a] *Department of Chemistry, Anhui University, Hefei, Anhui, 230601, China. E–mail: clj@ustc.edu.*

† Electronic Supplementary Information (ESI) available: The atomic coordinates (in Å) of the global minimum and low-energy structures of $(AuL)_n$ (L = Cl, SH, SCH3, PH2, P(CH3)2, n = 1-13) clusters. See DOI: 10.1039/x0xx00000x

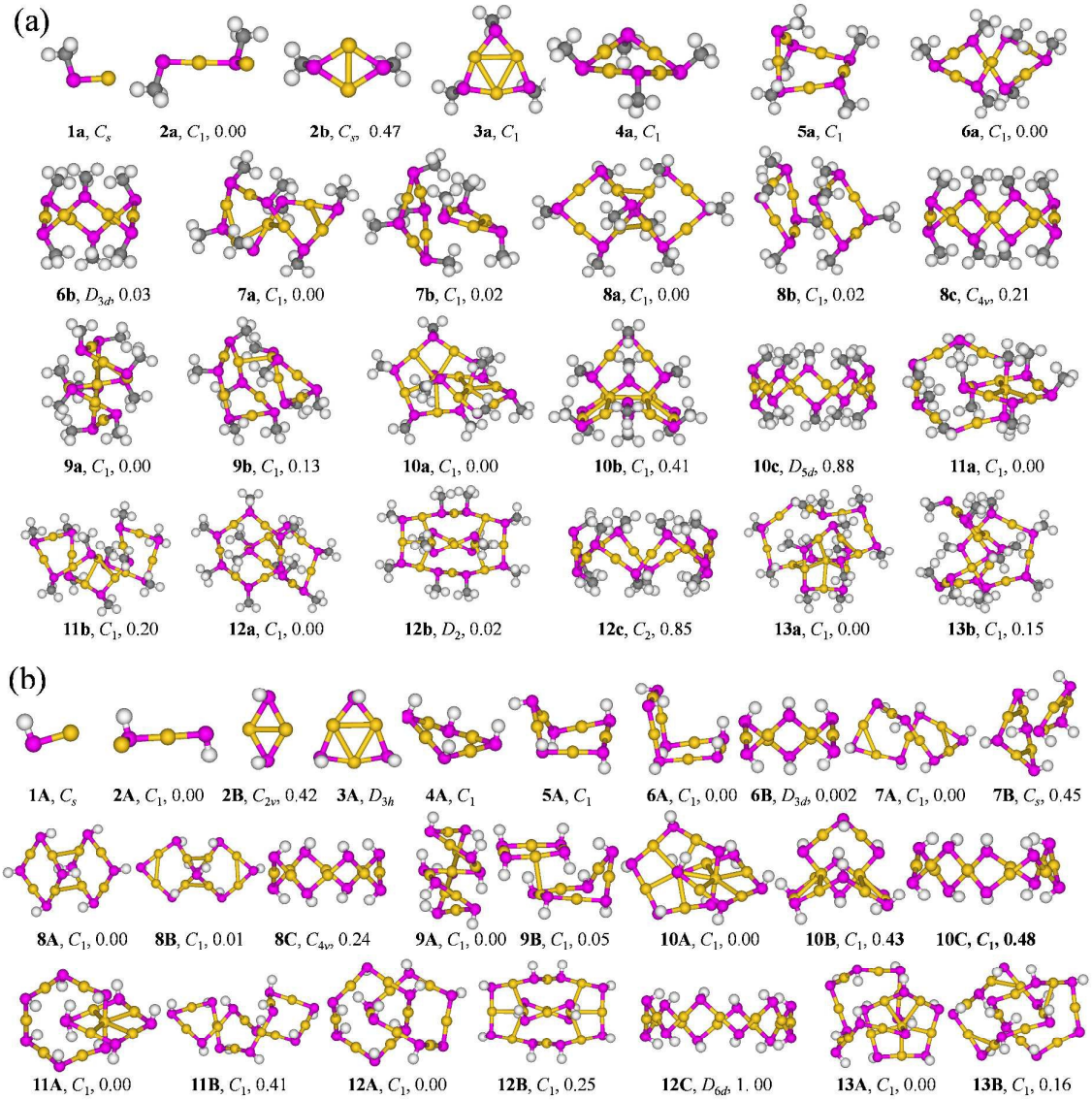

Fig. 1 Optimized geometries of (a) $(AuSCH_3)_n$ and (b) $(AuSH)_n$ (n = 1-13) clusters at TPSSh/6-311G* (S, H, C) and Lanl2TZ(f) (Au) level, Au-yellow, S-purple, H-white, C-gray.

The aforementioned ligand effects are mainly those on $Au_{102}(SR)_{44}$ and $Au_{25}(SR)_{18}$ clusters with gold-to-ligand ratio greater than 1:1. Previous studies also made some progress in the homoleptic type of -SR and -PR_2 groups protected Au clusters. The cyclic oligomers of $[Au(PR_2)]_n$ (n = 3, 4, 6) have been synthesized and characterized.[35-37] The lowest-energy isomers of $(AuCl)_n$ (n = 3-6) clusters are also found to be cyclic arrangements.[38] The synthetic $Au_{10}(SR)_{10}$ and $Au_{12}(SR)_{12}$ clusters were found to be composed by two interpenetrating pentagons and hexagons, respectively.[39] Gronbeck and co-workers explored the low-lying structures of $(AuSR)_n$ with n = 2-12 and predicted a transition from planar rings to crown structures.[40] The structures of $(AuSR)_n$ (n = 6-12) clusters were relocated by DFT and MP2 methods and the work discovered a new structural family of double helical conformation.[41]

Despite significant progresses in the area of Au_mL_n clusters, size evolution and ligand effects on $(AuL)_n$ clusters with Au-to-L ratio of 1:1 still lack systematic investigation because of limited experimental data on the structures. To the best of our knowledge, there are rare literatures on ligand effects of $(AuL)_n$ clusters. Herein we seek to investigate the ligand effects on the size evolution of $(AuL)_n$ clusters, with n = 1-13, L = Cl, SH, SCH_3, PH_2 and $P(CH_3)_2$. DFT method combined with genetic algorithm (GA) is used to locate the global minimum (GM) structures of the clusters. To explore the origin of ligand effects, the polarity of bonds, aurophilicity and binding energies of the clusters are also discussed.

II. Computational Details

The global minimum search for the $(AuL)_n$ clusters is carried out using GA coupled with DFT, which has been successfully applied in the structural prediction of a number of systems.[42-45] GA is an optimization strategy inspired by the Darwinian evolution that mimics the process of natural selection.[46-48] This strategy is routinely used to generate useful solutions to optimization and search problems. GA belongs to the larger class of evolutionary algorithms, which generate solutions to optimization problems using techniques inspired by natural evolution, such as inheritance, mutation, selection, and crossover. Starting with a population of candidate structures, we relax these candidates to the nearest local minimum. Using the relaxed energies as the criteria, a fraction of the population is selected as "parents". The next generation of candidate structures is the structure matching the "parents". The progress is repeated until the GMs is located.[49] The TPSSh functional[50] is selected for DFT calculation, which has been proven reliable in prediction of the ligand-protected Au nanoclusters.[51, 52] The unbiased global search of the potential energy surface at the DFT level is very time-consuming. Thus, in the global search procedure, we choose small basis sets, 3-21G for Cl, S, P, C, H and Lanl2MB for Au, in DFT calculations for saving time. With a small basis set, all the possible motifs can be found, but the energy sequences of various isomers are different. Then, the obtained low-lying geometries are fully relaxed at the TPSSh/6-311G*/LANL2TZ(f) level after global optimization. The normal mode frequencies are also computed at the same level for all structures to ensure that they belong to minima, and all the minima are verified by the absence of imaginary frequency. All DFT calculations are carried out using the GAUSSIAN 09 package.[53]

III. Results and Discussion

In this work, the GMs and low-lying isomers of $(AuL)_n$ (L = Cl, SH, SCH_3, PH_2 and $P(CH_3)_2$, n = 1-13) are located at the TPSSh/6-31G*/Lanl2DZ level, which include single-ring, helical, crown, catenane and double-ring structures. Then to investigate size evolution and ligand effects, the average binding energies, aurophilicity and the polarity of bonds are discussed.

1. Geometric structures

We first introduce the geometric structures of $(AuSCH_3)_n$ (n = 1-13) clusters (Fig. 1a), which have been reported before for n = 2-12.[26,27] All the known GMs are reproduced in our work. **2a** is a fold line, which is 0.47 eV lower in energy than the previous rhombic isomer. When n = 3-9, the single rings are the GMs. However, **3a** is a planar single ring, while **4a** and **5a** are twisted single rings. The GMs are all helical structures at n = 6-9. In particular, **8a** and **8b** are competitive isomers, and **8a** lies only 0.02 eV lower in energy than **8b** (a double-ring structure consisting of two four-membered rings). When n = 10-12, the GMs are all catenane structures consisting of two interpenetrating five-/six-membered rings. Worth noting is that **12b** and **12a** are nearly degenerated in energy.

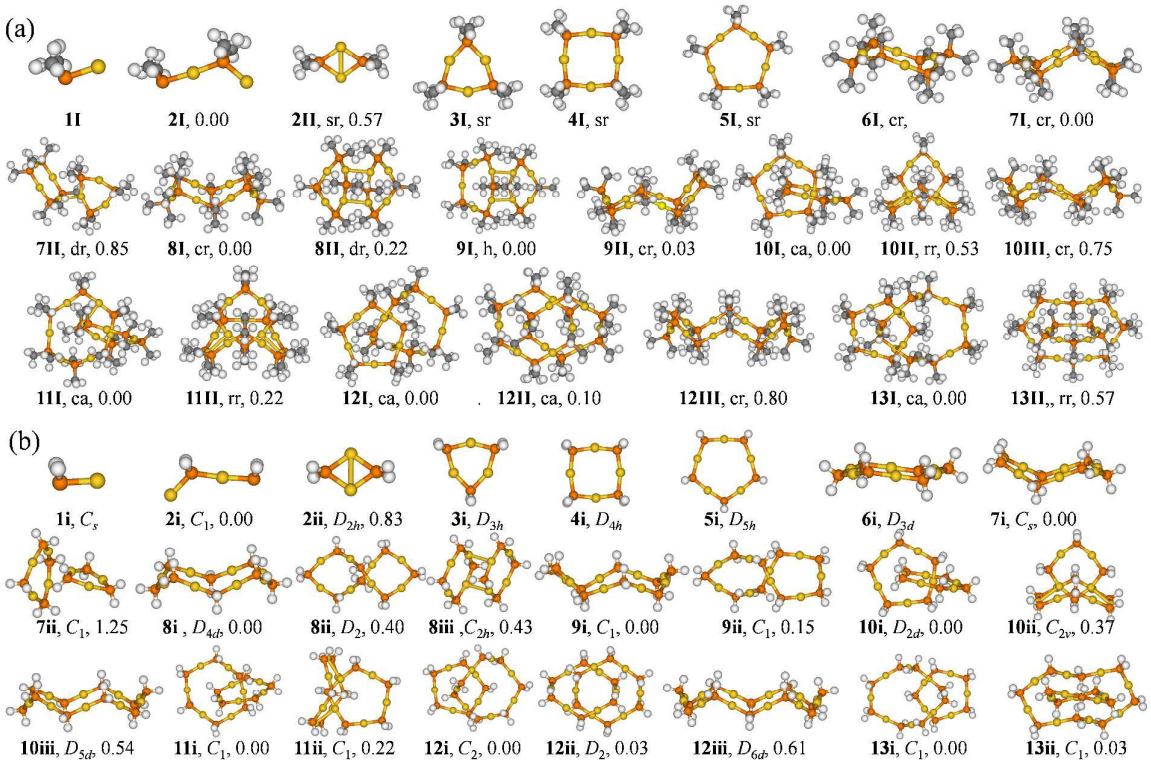

Fig. 2 Optimized geometries of (a) $[AuP(CH_3)_2]_n$ and (b) $(AuPH_2)_n$ (n = 1-13) clusters at TPSSh/6-311G* (P, C, H) and Lanl2tz(f) (Au) level, Au-yellow, P-orange, H-white, C-gray. The labels are sr: single ring, cr: crown, dr: double ring, h: helix, ca: catenane.

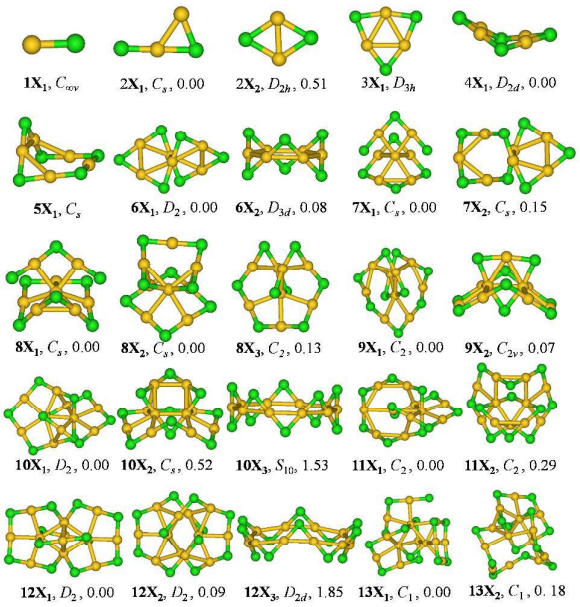

Fig. 3 Optimized geometries of $(AuCl)_n$ (n = 1-13) at TPSSh/6-311G* (Cl) and Lanl2tz(f) (Au) level, Au-yellow, Cl-green.

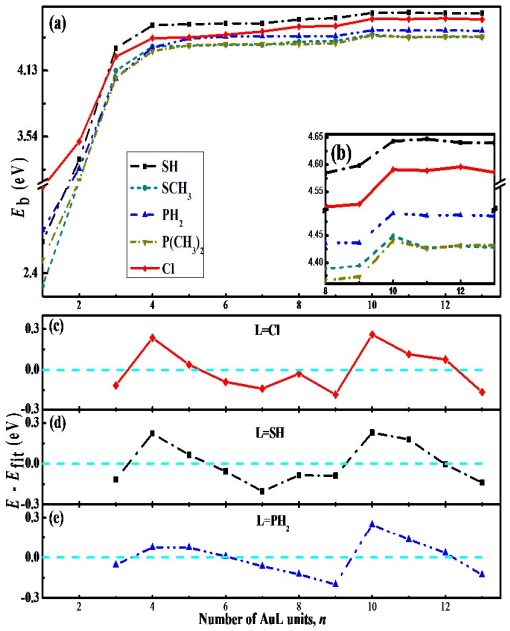

Fig. 4 (a) Binding energy of the GMs of $(AuL)_n$ (L = Cl, SH, SCH_3, PH_2, $P(CH_3)_2$) clusters as the function of cluster size n. (b) Enlarged binding energy of the GMs of $(AuL)_n$ (L = Cl, SH, SCH_3, PH_2, $P(CH_3)_2$) clusters in the 8-13 region. (c-e) Plots of the energetic gaps (E-E_{fit}) of the lowest-energy $(AuL)_n$ (L = Cl, SH, PH_2) clusters as a function of cluster size, where E is the total energy, and E_{fit} is a four-parameter fit of the GMs: $E_{fit} = a - b*n^{1/3} + c*n^{2/3} + d*n$ (related coefficient R > 0.999).

Interestingly, **12b** has a unique ring-at-ring structure (a small Au_4L_4 ring inserting into a large Au_8L_8 ring), which has not been reported before. **13a** is also a catenane structure, which is composed of five- and eight-membered interpenetrating rings. The crown isomers with high symmetries are also shown in Fig. 1a, which are lying much high in energy at large sizes.

In most calculations, the large -SR groups in experiments are often replaced by $-SCH_3$ group to reduce the computation cost.[54] Then, can the $-SCH_3$ group be further replaced by -SH group in calculations? Fig. 1b plots the GMs and low-energy isomers of $(AuSH)_n$ clusters. It can be seen that $(AuSH)_n$ clusters are in agreement with $(AuSCH_3)_n$ clusters in GM structures,except for n = 8, where the energy sequence changes slightly. The double-ring and helical structure are also competitive in energy at n = 8, where the former (**8A**) is 0.01 eV lower in energy for L = SH but is 0.02 eV higher in energy for L = SCH_3. Due to the great similarity between the structures of $(AuSH)_n$ and $(AuSCH_3)_n$, it can be expected that the -SR groups can be simplified directly to -SH group in calculations for structural prediction of $Au_m(SR)_n$ complexes.

To explore the ligand effects, we locate the GMs of $(AuL)_n$ clusters with $-SCH_3$ group replaced by $-P(CH_3)_2$ group. Fig. 2a displays the GMs and low-energy structures of $[(AuP(CH_3)_2]_n$ clusters. From the figure, we can see that the frameworks of the $(AuSCH_3)_n$ and $[(AuP(CH_3)_2]_n$ clusters are very similar. But the planar single rings are global minimum up to n = 5, and the GMs prefer crown structures at n = 6-8 in $[(AuP(CH_3)_2]_n$. Moreover, the GM of $[(AuP(CH_3)_2]_{12}$ (**12I**) is a catenane structure consisting of five- and seven-membered rings instead of two six-membered rings in $(AuSCH_3)_{12}$.

According to Fig. 2b, we can see that the GMs of $(AuPH_2)_n$ are very similar to those of $[AuP(CH_3)_2]_n$ clusters. The differences are that, the GM of $(AuPH_2)_9$ is a crown structure and the GM of $(AuPH_2)_{13}$ is a ring-at-ring structure (a small Au_5L_5 ring inserting into a large Au_8L_8 ring). Due to the great similarity between $(AuPH_2)_n$ and $[AuP(CH_3)_2]_n$, the large $-PR_2$ groups in experiments can be simplified by $-PH_2$ group in calculations.

Due to practical reasons, there is no report about the synthesis of the Cl-protected gold nanoclusters. However, sometimes the -SR and $-PR_2$ ligands can be replaced by -Cl group for theoretical computations to predict structures in calculations.[55, 56] The GMs and low-lying structures of $(AuCl)_n$ clusters are given in Fig. 3. It can be seen that $(AuCl)_n$ clusters also have certain similarities with $(AuSCH_3)_n$ clusters in the structures. When n ranges from 3-5, the GMs present single rings, while those of n = 6 and 9 are helical structures. When n = 10 and 11, the GMs are catenane structures. Obviously, the GMs have unique structures at n = 7, 8, 12, 13 and the energy sequences also change compared with $(AuSCH_3)_n$ clusters. Concretely, $\mathbf{7X_1}$ is a double-ring structure consisting of three- and four-membered rings, and one edge of the three-membered ring is broken. Similarly, the three-membered rings in $\mathbf{8X_1}$ is broken to make Au atoms close to each other. $\mathbf{12X_1}$ is a ring at ring structure (a Au_4Cl_4 ring inserting into a Au_8Cl_8 ring), however, linearity of two Cl-Au-Cl edges in the Au_8Cl_8 unit is broken to 110°. $\mathbf{13X_1}$ is an irregular structure with a broken four-membered interpenetrating ring. Reasons for the serious breaking of the Cl-Au-Cl linearity at n = 7, 8, 12 and 13 are to have more Au···Au contacts.

Table I Comparison of bond angles for the monocyclic structures of $(AuCl)_n$, $(AuSH)_n$ and $(AuPH_2)_n$ clusters.

N	$(AuCl)_n$		N	$(AuSH)_n$		N	$(AuPH_2)_n$	
	Au-Cl-Au(°)	Cl-Au-Cl(°)		Au-S-Au(°)	S-Au-S(°)		Au-P-Au(°)	P-Au-P(°)
$2X_2$	64.2	115.8	2B	65.4	114.6	2ii	73.4	106.6
$3X_1$	74.5	165.5	3A	77.2	162.8	3i	88.4	151.6
$4X_1$	87.4	177.4	4A	87.5	178.2	4i	104	166.0
$5X_1$	78.7~95.8	177.7	5A	94.6	177.3	5i	114.1	173.9
$6X_2$	79.8	178.5	6A	87.6	178.8	6i	119	177.7
$8X_3$	79.2	178.9	8C	88.1	178.2	8i	119.7	179.0
$10X_3$	79.2	179.1	10C	88.9	177.9	10iii	120	179.5
$12X_3$	79.2	179.3	12C	89.5	177.8	12iii	120.1	179.8

2. Binding energies

Based on the structural analysis above, it is found that $(AuL)_n$ clusters with different ligand types show certain differences in the structures. To explore ligand effects on stability, the average binding energies (E_b) per AuL unit of each GM clusters are calculated, which is defined as: $E_b = (n*E_{Au} + n*E_L - E_{(AuL)n})/n$, wherein E_{Au}, E_L and $E_{(AuL)n}$ are the energies of Au, L and $(AuL)_n$, respectively. Fig. 4a compares the E_bs as a function of cluster sizes of the five ligands. It is clearly seen that there is an increment in E_b as the successive addition of one AuL unit. For L = Cl, SH and SCH_3, E_b increases quickly up to n = 3, and then converges at n = 4. For L = PH_2 and $P(CH_3)_2$, E_b increases quickly with n up to 4, and then converges at n = 5. For each ligand, E_b reaches the highest value at n = 10 (Fig. 4b), indicating magic stability of the structure with two interpenetrating five-membered rings. From the curves of E_b, the order of stability for each ligand should be: SH > Cl > PH_2 > SCH_3 > $P(CH_3)_2$. $(AuSH)_n$ is obviously more stable than $(AuSCH_3)_n$ at a large size, which may be due to the weak hydrogen bond (S···H-S) in the former. For L = PH_2, SCH_3 and $P(CH_3)_2$, the small stability differences may be due to the steric effects of -CH_3 group.

To show the size evolution more clearly, for L = Cl, SH, PH_2, relative energies of the total binding energies (E) and its fitting (E_{fit}) are plotted in Fig. 4c-e in a manner that emphasizes particular stable minima or "magic numbers". In such curves, positive peaks correspond to more stable structures. It can be seen that, for each ligand, there are two pronounced peaks at n = 4 and 10, indicating that $(AuL)_4$ and $(AuL)_{10}$ are more stable than their neighbors. For L = Cl, there is a small peak at n = 8, indicating the stability of the double-ring $(AuCl)_8$ cluster. It should be noted that the stability of $(AuPH_2)_5$ is similar to that of $(AuPH_2)_4$, manifesting the stability of five-membered ring. This results in the highest relative stability of $(AuPH_2)_{10}$ among the three ligands.

3. Aurophilicity

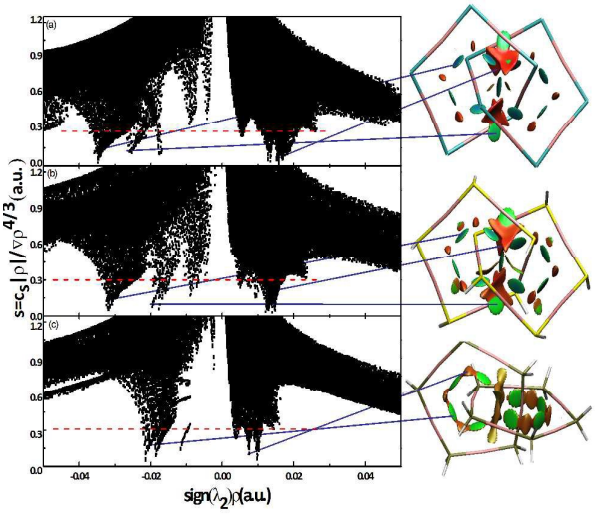

Fig. 5 Plots of the reduced density gradient versus the electron density multiplied by the sign of the second Hessian eigenvalue (left) and NCI isosurfaces at s = 0.30 (right) for the global minimum structures of (a) $(AuCl)_{10}$, (b) $(AuSH)_{10}$ and (c) $(AuPH_2)_{10}$.

Previous studies suggested that the strong Au···Au aurophilic interaction was responsible for the stability of closed-chain gold thiolate $[Au(SC_6H_4\text{-}p\text{-}CMe_3)]_{10}$,[37, 38] and the catenane structures can give rise to the largest number of close Au···Au contacts, resulting in lower energies. For large cluster sizes (n ≥ 10) of these systems, it is found that most of the GMs are catenane structures. For L = Cl, the linearity of Cl-Au-Cl bonds is broken at n = 7, 8 and 12 to have more Au···Au contacts due to aurophilicity. However, aurophilicity is a kind of weak noncovalent interaction, and cannot be studied directly by the natural bonding orbital methods. Here, we use the noncovalent interaction (NCI) index approach to detect aurophilicity based on the electron density and its derivatives,[57, 58] which has been successfully applied to investigate the aurophilic interaction in $(Au_2S)_n$ clusters.[59] The NCI studies are carried out using Multiwfn package,[60] and the NCI isosurface images are created using VMD.[61] The NCI index is based on the reduced density gradient, s, and the electron density, ρ,

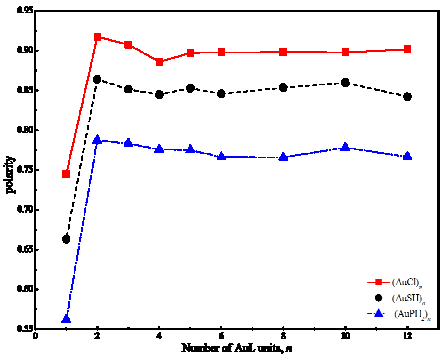

Fig. 6 Polarity of Au-L bond in monocyclic $(AuL)_n$ clusters (L = Cl, SH, PH_2) as the function of cluster size n.

where

$$s = \frac{1}{2(3\pi^2)^{1/3}} \frac{|\nabla\rho|}{\rho^{4/3}}$$

and it permits to highlight interactions characterized by a low-density regime. To distinguish different types of interactions, the second Hessian eigenvalue (λ_2) can be used as a sign, which can be either positive or negative.

Fig. 5 plots the reduced density gradient (*s*) versus the electron density (ρ) multiplied by the sign of λ_2 and the low-gradient (*s* = 0.30 au) NCI isosurfaces of the three typical structures $(AuCl)_{10}$ (**10X$_1$**), $(AuSH)_{10}$ (**10A**) and $(AuPH_2)_{10}$ (**10i**). From the left part of Fig. 5, the low density, low-gradient spikes lie at about sign $(\lambda_2)\rho$ = -0.035 au for $(AuCl)_{10}$, -0.032 au for $(AuSH)_{10}$ and -0.020 au for $(AuPH_2)_{10}$, respectively, which represent strong noncovalent attractions and more negative spikes represent stronger attractions (Au···Au aurophilic interactions between the central gold atoms in each ring and those on the periphery). The Au···Au aurophilic interactions can be viewed directly from the NCI isosurfaces in the right part of Fig. 5, where the darkness of the color indicates the strength of the Au···Au aurophilicity (Cl > SH > PH_2). Besides, the average Au···Au distances in $(AuCl)_{10}$, $(AuSH)_{10}$ and $(AuPH_2)_{10}$ clusters are 2.96 Å, 3.04 Å, 3.34 Å, respectively, which agree well with the relative strength of Au···Au aurophilic interactions within them. Moreover, for $(AuCl)_{10}$ and $(AuSH)_{10}$ clusters, there are smaller spikes at about sign $(\lambda_2)\rho$ = -0.025 au and -0.020 au, respectively, which represent another Au···Au aurophilic interactions (between gold atoms around the periphery as viewed in the NCI isosurfaces). The average Au···Au distances between gold atoms around the periphery are 3.11 Å and 3.30 Å for L = Cl and SH, respectively, in agreement with their relative strength. In particular, both $(AuSH)_{10}$ and $(AuPH_2)_{10}$ have low density spikes at sign $(\lambda_2)\rho$ = -0.020 au, and the average Au···Au distances are close to each other. It further shows that the Au···Au distance is in agreement with the relative strength of Au···Au aurophilic interactions. In addition, the spikes at positive values represent steric interactions between the two rings, which are the red regions of isosurfaces. By comparison, Figures 5a and 5b dealing with $(AuCl)_{10}$ and $(AuSH)_{10}$, respectively, are almost the same. This trend is also somewhat reflected in the calculated geometrical parameters reported in Table 1, and also in the average Au…Au distances of 2.96 and 3.04 Å. However, the $(AuPH_2)_{10}$ cluster shows differences in all these properties.

4. Polarity and bond angles

Previous comparisons show that the aurophilicity in $(AuCl)_n$ cluster is the strongest, followed by those in $(AuSH)_n$ and $(AuPH_2)_n$. As we know, the order for polarity of the Au-L bonds is: Au-Cl > Au-SH > Au-PH_2. Thus, the aurophilicity may be affected by the polarity of Au-L bonds. To verify the Au-L bond polarity in the different homoleptic gold clusters, natural bonding orbital (NBO) analysis[62-64] is performed on the single-ring structures. The results are shown in Fig. 6, where the polarity of a Au-L bond is represented as the percentage of the shared electron pairs owing to L. For $(AuL)_n$ (*n* = 1), Au and L atoms supply one electron each to form one Au-L bond, and the polarity of Au-Cl, Au-S and Au-P bonds are 0.75, 0.66, 0.56, respectively, indicating that the charge is polarized towards L. When *n* ≥ 2, each L contributes three electrons and each Au contributes one electron to form 2*n* Au-L bonds, so the polarity increases suddenly at *n* = 2, and then levels off at *n* > 2. Due to the larger electronegativity difference between Au and Cl atoms, the polarity of the Au-Cl bonds is stronger than Au-S and Au-P bonds which are in accordance with the relative strength of Au···Au aurophilic interactions. Moreover, stronger polarity can result in weaker covalency which can make it easier for the linearity of L-Au-L bonds to be broken. For L = Cl, because of the strongest polarity and aurophilicity, the linearity of Cl-Au-Cl bonds is the easiest to be broken for more Au···Au aurophilic contacts, which is found in the GMs of $(AuCl)_7$, $(AuCl)_8$, $(AuCl)_{12}$ and $(AuCl)_{13}$.

Moreover, due to the difference in polarity for Au-L bonds, the preferred angles of Au-L-Au bonds are different which further affects the structures. Table I compares the changes in Au-L-Au angles for the monocyclic structures of these three systems. For small cluster sizes, the Au-Cl-Au, Au-S-Au and Au-P-Au angles show substantial contractions, respectively, from the ideal 79°, 89° and 120°. The Au-Cl-Au angles reach the ideal values at *n* = 3-4 for L = Cl, *n* = 4 for L = SH, and *n* = 5-6 for L = PH_2. Thus, $(AuCl)_4$, $(AuSH)_4$ and $(AuPH_2)_5$ with ideal Au-L-Au angles are more stable than their neighbors.

IV. Conclusions

In present work, the size evolution and ligand effects of $(AuL)_n$ clusters with *n* = 1-13, L = Cl, SH, SCH_3, PH_2, $P(CH_3)_2$, are investigated using the method combining the GA with DFT. The GMs of $(AuSCH_3)_n$ shift from single rings at *n* = 2-9 to catenane structures at *n* ≥ 10, which are in agreement with previous works. Besides, a new folding way (ring-at-ring) is revealed in the GMs at *n* = 12-13. When the ligands are SH, PH_2 and $P(CH_3)_2$, the structural features are roughly similar to that of $(AuSCH_3)_n$. Thus, -SCH_3 group can be replaced by -SH group, which points to a way to predict the structures of $Au_m(SR)_n$ by exploring $Au_m(SH)_n$ clusters. Similarly, the large -PR_2 groups in experiments can be directly simplified by -PH_2 group in calculations. For L = Cl, most of the GMs are also single rings and catenane structures, but the linearity of Cl-Au-Cl is broken at *n* = 7, 8 and 12 to have more Au···Au contacts due to the aurophilicity.

NCI method reveals that the aurophilicity in $(AuCl)_n$ cluster is the strongest, followed by those in $(AuSH)_n$ and $(AuPH_2)_n$, which is accompanied by the lengthening of Au···Au distances. The polarity of Au-L bonds is the strongest for L = Cl among these three ligands, which is in accordance with the relative strength of Au···Au aurophilic interactions and further results in breaking of the Cl-Au-Cl linearity at some GM structures. The polarity could also affect the preference of Au-L-Au angles and further results in the difference of structures. $(AuCl)_4$, $(AuSH)_4$ and $(AuPH_2)_5$ with ideal Au-L-Au angles are more stable than their neighbors. This results in the highest relative stability of $(AuPH_2)_{10}$ among the three ligands.

Ligand effects are frequently viewed in the experimentally produced ligand-protected Au clusters. Taking $(AuL)_n$ clusters as examples, this work try to answer the question how ligands affect the structures. The origin is the polarity of Au-L bond, which results in gaps in the strength of Au···Au aurophilic interactions and in the preferred Au-L-Au angles.

Acknowledgments

This work is supported by the National Natural Science Foundation of China (Grant Nos. 21273008, 21573001). The calculations are carried out on the High-Performance Computing Center of Anhui University.

References

1. B. K. Juluri, Y. B. Zheng, D. Ahmed, L. Jensen and T. J. Huang, *J. Phys. Chem. C*, 2008, **112**, 7309-7317.
2. Y. B. Zheng, L. Jensen, W. Yan, T. R. Walker, B. K. Juluri, L. Jensen and T. J. Huang, *J. Phys. Chem. C*, 2009, **113**, 7019-7024.
3. A. Tcherniak, S. Dominguez Medina, W. S. Chang, P. Swanglap, L. S. Slaughter, C. F. Landes and S. Link, *J. Phys. Chem. C*, 2011, **115**, 15938-15949.
4. M. Draper, I. M. Saez, S. J. Cowling, P. Gai, B. Heinrich, B. Donnio, D. Guillon and J. W. Goodby, *Adv. Funct. Mater.*, 2011, **21**, 1260-1278.
5. T. V. Basova, R. G. Parkhomenko, I. K. Igumenov, A. Hassan, M. Durmus, A. G. Gurek and V. Ahsen, *Dyes Pigm.*, 2014, **111**, 58-63.
6. H. C. Weissker, R. L. Whetten and X. Lopez-Lozano, *Phys. Chem. Chem. Phys.*, 2014, **16**, 12495-12502.
7. Q. Hao, B. K. Juluri, Y. B. Zheng, B. Wang, I. K. Chiang, L. Jensen, V. Crespi, P. C. Eklund and T. J. Huang, *J. Phys. Chem. C*, 2010, **114**, 18059-18066.
8. P. D. Jadzinsky, G. Calero, C. J. Ackerson, D. A. Bushnell and R. D. Kornberg, *Science*, 2007, **318**, 430-433.
9. J. Akola, M. Walter, R. L. Whetten, H. Hakkinen and H. Grönbeck, *J. Am. Chem. Soc.*, 2008, **130**, 3756-3757.
10. H. Hakkinen, R. Barnett and U. Landman, *Phys. Rev. Lett.*, 1999, **82**, 3264.
11. H. Qian, Y. Zhu and R. Jin, *ACS Nano*, 2009, **3**, 3795-3803.
12. Y. Pei, Y. Gao and X. C. Zeng, *J. Am. Chem. Soc.*, 2008, **130**, 7830-7832.
13. S. Knoppe, A. C. Dharmaratne, E. Schreiner, A. Dass and T. Bürgi, *J. Am. Chem. Soc.*, 2010, **132**, 16783-16789.
14. O. Lopez-Acevedo, H. Tsunoyama, T. Tsukuda and C. M. Aikens, *J. Am. Chem. Soc.*, 2010, **132**, 8210-8218.
15. Y. Pei, R. Pal, C. Liu, Y. Gao, Z. Zhang and X. C. Zeng, *J. Am. Chem. Soc.*, 2012, **134**, 3015-3024.
16. M. Zhu, H. Qian and R. Jin, *J. Phys. Chem. Lett.*, 2010, **1**, 1003-1007.
17. H. Qian and R. Jin, *Chem. Mater.*, 2011, **23**, 2209-2217.
18. S. Malola and H. Hakkinen, *J. Phys. Chem. Lett.*, 2011, **2**, 2316-2321.
19. H. Qian and R. Jin, *Nano Lett.*, 2009, **9**, 4083-4087.
20. J. Z. Sexton and C. J. Ackerson, *J. Phys. Chem. C*, 2010, **114**, 16037-16042.
21. C. Yi, M. A. Tofanelli, C. J. Ackerson and K. L. Knappenberger Jr, *J. Am. Chem. Soc.*, 2013, **135**, 18222-18228.
22. M. Azubel, J. Koivisto, S. Malola, D. Bushnell, G. L. Hura, A. L. Koh, H. Tsunoyama, T. Tsukuda, M. Pettersson and H. Hakkinen, *Science*, 2014, **345**, 909-912.
23. A. Das, C. Liu, H. Y. Byun, K. Nobusada, S. Zhao, N. Rosi and R. Jin, *Angew. Chem.*, 2015, **127**, 3183-3187.
24. S. Chen, S. Wang, J. Zhong, Y. Song, J. Zhang, H. Sheng, Y. Pei and M. Zhu, *Angew. Chem., Int. Ed.*, 2015, **54**, 3145-3149.
25. R. Guo and R. W. Murray, *J. Am. Chem. Soc.*, 2005, **127**, 12140-12143.
26. Y. Negishi, N. K. Chaki, Y. Shichibu, R. L. Whetten and T. Tsukuda, *J. Am. Chem. Soc.*, 2007, **129**, 11322-11323.
27. G. E. Johnson, A. Olivares, D. Hill and J. Laskin, *Phys. Chem. Chem. Phys.*, 2015, **17**, 14636-14646.
28. A. Tlahuice-Flores, R. L. Whetten and M. Jose-Yacaman, *J. Phys. Chem. C*, 2013, 117, 20867-20875.
29. J. Jung, S. Kang and Y. K. Han, *Nanoscale*, 2012, **4**, 4206-4210.
30. Y. Gao, *J. Phys. Chem. C*, 2013, **117**, 8983-8988.
31. Q. Tang, R. Ouyang, Z. Tian and D. E. Jiang, *Nanoscale*, 2015, **7**, 2225-2229.
32. T. W. Ni, M. A. Tofanelli, B. D. Phillips and C. J. Ackerson, *Inorg. Chem.*, 2014, **53**, 6500-6502.
33. E. Pohjolainen, H. Hakkinen and A. Clayborne, *J. Phys. Chem. C*, 2015, **119**, 9587-9594.
34. J. Zhong, X. Tang, J. Tang, J. Su and Y. Pei, *J. Phys. Chem. C*, 2015, **119**, 9205-9214.
35. D. M. Stefanescu, H. F. Yuen, D. S. Glueck, J. A. Golen and A. L. Rheingold, *Angew. Chem., Int. Ed.*, 2003, **42**, 1046-1048.
36. D. M. Stefanescu, H. F. Yuen, D. S. Glueck, J. A. Golen, L. N. Zakharov, C. D. Incarvito and A. L. Rheingold, *Inorg. Chem.*, 2003, **42**, 8891-8901.
37. D. M. Stefanescu, D. S. Glueck, R. Siegel and R. E. Wasylishen, *Langmuir*, 2004, **20**, 10379-10381.
38. F. Rabilloud, *J. Comput. Chem.*, 2012, **33**, 2083-2091.
39. M. R. Wiseman, P. A. Marsh, P. T. Bishop, B. J. Brisdon and M. F. Mahon, *J. Am. Chem. Soc.*, 2000, 122, 12598-12599.
40. H. Gronbeck, M. Walter and H. Hakkinen, *J. Am. Chem. Soc.*, 2006, **128**, 10268-10275.
41. N. Shao, Y. Pei, Y. Gao and X. C. Zeng, *J. Phys. Chem. A*, 2009, **113**, 629-632.
42. Y. Yuan and L. Cheng, *J. Chem. Phys.*, 2012, **137**, 044308.
43. Y. Yuan and L. Cheng, *Int. J. Quantum Chem.*, 2012, **113**, 1264-1271.
44. Y. Yuan, L. Cheng and J. Yang, *J. Phys. Chem. C*, 2013, **117**, 13276-13282.
45. L. Li and L. Cheng, *J. Chem. Phys.*, 2013, **138**, 094312.
46. R. L. Johnston, *Dalton Trans.*, 2003, 4193-4207.
47. A. Shayeghi, D. Götz, J. Davis, R. Schaefer and R. L. Johnston, Phys. Chem. Chem. Phys., 2015, 17, 2104-2112.
48. D. M. Deaven and K. M. Ho, *Phys. Rev. Lett.*, 1995, **75**, 288-291.
49. S. Hamad, C. Catlow, S. Woodley, S. Lago and J. Mejias, *J. Phys. Chem. B*, 2005, **109**, 15741-15748.
50. M. Mantina, R. Valero and D. G. Truhlar, *J. Chem. Phys.*, 2009, **131**, 64706.
51. Y. K. Shi, Z. H. Li and K. N. Fan, *J. Phys. Chem. A*, 2010, **114**, 10297-10308.
52. L. Cheng, Y. Yuan, X. Zhang and J. Yang, *Angew. Chem., Int. Ed.*, 2013, **52**, 9035-9039.
53. M. Frisch, G. Trucks, H. B. Schlegel, G. Scuseria, M. Robb, J. Cheeseman, G. Scalmani, V. Barone, B. Mennucci and G. Petersson, *Gaussian 09, Revision B. 01, Gaussian Inc., Wallingford, CT*, 2010.
54. J. A. Howell, *Polyhedron*, 2006, **25**, 2993-3005.
55. D. E. Jiang and M. Walter, *Nanoscale*, 2012, **4**, 4234.
56. Z. M. Tian and L. J. Cheng, *Phys. Chem. Chem. Phys.*, 2015, **17**, 13421.
57. E. R. Johnson, S. Keinan, P. Mori-Sanchez, J. Contreras-Garcia, A. J. Cohen and W. Yang, *J. Am. Chem. Soc.*, 2010, **132**, 6498-6506.
58. J. Contreras-García, E. R. Johnson, S. Keinan, R. Chaudret, J. P. Piquemal, D. N. Beratan and W. Yang, *J. Chem. Theory Comput.*, 2011, **7**, 625-632.
59. Y. Q. Feng and L. J. Cheng, *RSC Adv.*, 2015, **5**, 62543.
60. T. Lu and F. Chen, *J. Comput. Chem.*, 2012, **33**, 580-592.
61. W. Humphrey, A. Dalke and K. Schulten, *J. Mol. Graph.*, 1996, **14**, 33-38.
62. J. Foster and F. Weinhold, *J. Am. Chem. Soc.*, 1980, **102**, 7211-7218.

63. F. Weinhold and C. R. Landis, *Valency and bonding: a natural bond orbital donor-acceptor perspective*, Cambridge University Press, Cambridge, 2005.
64. A. E. Reed, L. A. Curtiss and F. Weinhold, *Chem. Rev.*, 1988, **88**, 899-926.

Table of Contents Entry

Size evolution on the global minimum structures of $(AuCl)_n$ clusters at n = 1-13